Stress-Induced Anisotropy of Small Strain Shear Modulus in Saturated and Unsaturated Cohesive Soils

Hirofumi Toyota[1], Ngoc Bao Le [2], and Susumu Takada[3]

[1] *Professor, Dept. of Civil and Environmental Eng., Nagaoka University of Technology, Japan*
(E-mail: toyota@vos.nagaokaut.ac.jp)
[2] *Engineer, Kiso-Jiban Consultants Co., Ltd., Japan*
(E-mail: le.ngocbao@kiso.co.jp)
[3] *Technical staff, Dept. of Civil and Environmental Eng., Nagaoka University of Technology, Japan*
(E-mail: stakada@konomi.nagaokaut.ac.jp)

ABSTRACT

Cohesive soils in nature have been existed under anisotropic stress conditions: Embankment produces an additional vertical load in the ground just under the embankment, while producing an additional horizontal load in the ground a little away from the embankment. This study investigates stress-induced anisotropic effects on small strain shear modulus in saturated and unsaturated cohesive soils. A triaxial apparatus installed local small strain (LSS) measurement devices and bender elements (BEs) was used to measure the small strain shear modulus. LSS and BE tests were conducted using specimens normally consolidated under constant effective stress p'=300 kPa or net mean stress p_{net}=300 kPa with different stress ratios, represented as $K= \sigma'_h/\sigma'_v$ for saturated soils and $K_{net} = (\sigma_h–u_a)/(\sigma_v–u_a)$ for unsaturated soils. The results demonstrated that K-consolidation under constant p' produces large differences in the initial shear modulus G_0 in saturated cohesive soil, but K_{net} slightly affects G_0 in unsaturated cohesive soil because of the strong matric suction effects. Finally, G_0 was normalized successfully considering the effects of void ratio e and stress ratio K and K_{net}.

Key words: bender element, induced anisotropy, local small strain, shear modulus, unsaturated soil

1. INTRODUCTION

The natural ground initially exhibits an anisotropic stress state of the K_0 condition after the natural sedimentation. Since then, the ground has had complicated stress histories through natural and artificial processes: tectonic movement, landslides, and construction works. Stress-induced anisotropy, which is induced by application of the anisotropic stress state, was first introduced by Casagrande and Corrilo (1944). It has since been recognized as an important mechanical property,

especially for cohesive soils.

The small strain shear modulus plays a crucial role for design tasks related to ground structures under static and/or dynamic loading conditions. Regarding the cohesive soils, Rampello et al. (1997), Chien and Oh (2002), and Hao and Lok (2008) reported that the shear modulus is greater in an anisotropic stress condition than that with isotropic stress consolidation. Mitaritona et al. (2014) considered the effects of both inherent anisotropy and induced anisotropy by investigating the ratio G_{hh}/G_{vh} under different stress-paths $\eta = q/p'$, indicating $\eta = 0$ (isotropic) and $\eta \neq 0$ (anisotropic). They demonstrated for clay that the ratio G_{hh}/G_{vh} increases from 1.0 at an isotropic stress condition to 1.2 at $\eta = 0.8$. Ng et al. (2009) found shear modulus anisotropy for unsaturated soils. They proved that $G_{0(hh)}/G_{0(vh)}$, where $G_{0(hh)}$ and $G_{0(vh)}$ respectively represent the shear modulus in the horizontal and vertical directions, decreased significantly from 1.03 to 0.87 when η changed from 0 (isotropic condition) to 1 (anisotropic condition).

Although current achievements for the study of this kind are described above, more comprehensive studies are recommended to clarify the mechanism of anisotropic shear modulus induced by stress conditions. Therefore, a series of triaxial tests, including bender element (BE) tests and local small strain (LSS) tests were conducted using the saturated and unsaturated specimens consolidated at various $K=\sigma'_h/\sigma'_v$ and $K_{net}=(\sigma_h-u_a)/(\sigma_v-u_a)$ under the same mean effective stress $p'=(\sigma'_v+2\sigma'_h)/3$ and net mean stress $p_{net}=p-u_a$ of 300 kPa, respectively.

2. EXPERIMENTS

2.1. Testing Materials and Specimen Preparation

Yoneyama silt, whose grain size distribution and index properties are presented in Fig. 1, was used in the study. Dry Yoneyama silt was mixed with de-aired water with water content of 80 % to produce slurry. The vacuum was applied to remove air from the slurry in an acrylic cylindrical mold. Then, air pressure of 45 kPa was applied to the upper space of the piston in the mold. The soil block, its water content of about 40 %, was extracted from the mold after 2 days of one-dimensional consolidation. A cylindrical specimen of 125 mm height and 50 mm diameter was trimmed from the extracted soil block.

The drying portion of soil-water characteristic curves obtained from the pressure plate method is shown in Fig. 2. Constant isotropic confining stresses of p_{net}=100 kPa and p_{net}=300 kPa are applied to the specimens during the drying using a triaxial apparatus. From the results, the air entry values of the soil under p_{net}=100 kPa and p_{net}=300 kPa can be respectively detected as about 50 kPa and 150 kPa.

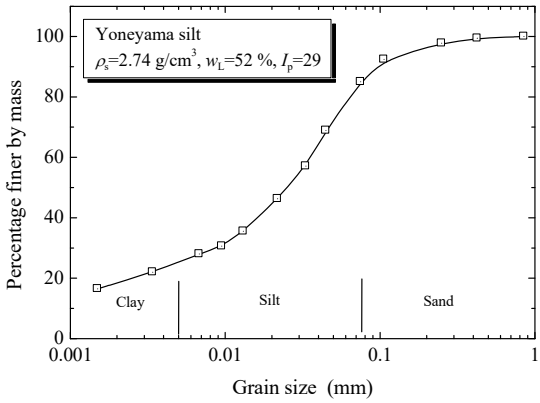

Figure 1. Grain size distribution curve and its physical properties

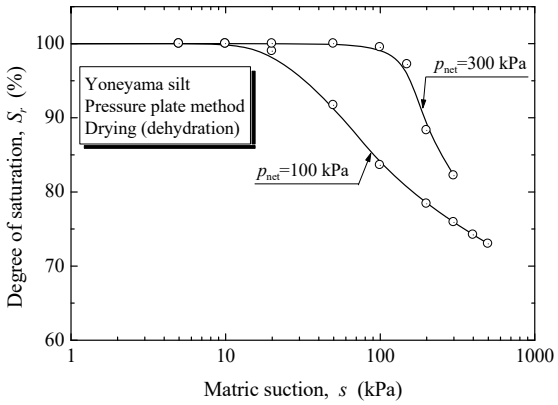

Figure 2. Soil-water characteristic curves (Toyota et al., 2017)

2.2. Testing Apparatus

A triaxial apparatus with integrated BEs and LSS measuring devices was used to measure the shear modulus at a small strain (e.g. Le et al., 2024). The LSS technique was developed to measure the smallest strain of 10^{-4} % using the proximity transducers with 0.2 μm resolution. Two targets were directly pasted onto the upper and the lower parts of specimen's side surface with distance of 80 mm for the vertical strain measurement. Two proximity transducers set on two individual columns respectively can be adjusted the distance between the transducers and the targets from outside of the triaxial cell. For horizontal strain measurements, a clamp device equipped with the proximity transducer and target was installed on the center of the specimen.

The BEs of 2.5 mm height, 12 mm length, and 1 mm thickness were attached to the top cap as a transmitter and the base pedestal as a receiver. Then BE tests were conducted to follow the standard of JGS 0544 (2020). Single sinusoidal waves with frequencies of 10, 15, 20 kHz at voltage ±10 V were used as the input wave. The start-to-start and the tip-to-tip methods were used to evaluate the shear wave velocity V_s.

2.3. Testing Methods

The stress paths are presented in Fig. 3. The testing procedure is described below.

1. Saturation and isotropic consolidation process: A specimen was saturated using the vacuum saturation procedure (Rad and Clough, 1984). Then, the cell water was removed while negative pore water pressure of –20 kPa was applied inside the specimen. The proximity transducers for LSS tests were installed. After re-supplying the cell water to the triaxial cell, the specimen was consolidated isotropically under confining pressure of 50 kPa. Back pressure of 200 kPa was applied to achieve a Skempton's B-value greater than 0.97 for the saturated soil.

2. Drained q-loading process: Maintaining p'=50 kPa, the specimen was sheared at an axial strain rate of 0.005%/min under a drained condition. The shearing continued until reaching a target deviator stress $q=\sigma'_v-\sigma'_h$, in which a certain $K=\sigma'_h/\sigma'_v$ of 0.35, 0.43, 0.6, 1.0, 1.5, 2.0, 3.0, and 3.5 was achieved. The test case at K of 3.5 was only conducted in BE tests of saturated soil because of testing apparatus limitations.
3. Drying process: q and $K_{net}=(\sigma_h-u_a)/(\sigma_v-u_a)$ were maintained while matric suction ($s=u_a-u_w$) of 400 kPa was applied to the specimen. This matric suction is greater than the air entry value (AEV) of the specimen (Fig. 2). During this process, p_{net}=50 kPa was also kept constant using the axis-translation technique. This process was continued until the water drained from the ceramic disc became less than 0.2 cm^3 per day. This process was skipped in the case of saturated soil.
4. K or K_{net}-consolidation process: K or K_{net} was kept constant with the same value set at the q-loading process. Also, p' or p_{net} was increased from 50 kPa to 300 kPa while maintaining K or K_{net}. Toyota et al. (2001) demonstrated that when the specimen of Yoneyama silt, which is prepared by the same method as this study, is isotropically consolidated with 100 kPa, it shows almost isotropic shear behavior. This indicates the structural anisotropy caused by the one-dimensional consolidation is largely eliminated by the isotropic consolidation with twice as much as the vertical stress of one-dimensional pre-consolidation. Hence, the application of p' or p_{net}=300 kPa will eliminate the effects of one-dimensional pre-consolidation with the vertical stress of 45 kPa on the subsequent shear behavior. The degree of saturation for unsaturated Yeneyama silt was about 80 % in this stage. Then, the BE test was conducted to obtain the initial shear modulus G_0 based on V_s of the specimen. K or K_{net}-consolidation was maintained for 24 h in all cases to make the aging effects even.

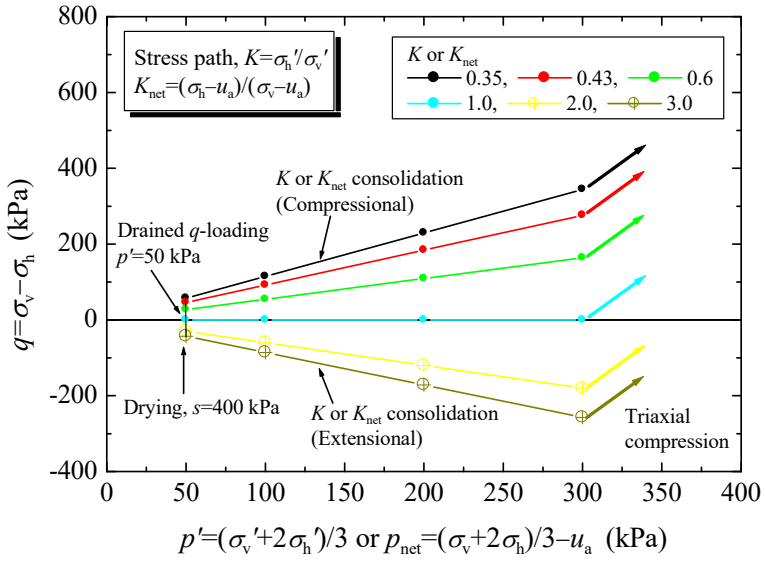

Figure 3. Stress paths during testing

5. Shearing process: Drained monotonic compression was conducted under constant cell pressure with an axial strain rate of 0.0025%/min. Shearing was continued until the shear strain ε_s exceeded 0.1%.

3. RESULTS

3.1. Effects of *K* or K_{net}-consolidation on the Secant Shear Modulus

Figure 4 presents the secant shear modulus G_{sec} versus the shear strain in LSS tests of saturated and unsaturated soils under triaxial compression. The value of G_{sec} is calculated as shown in equation (1).

$$G_{sec} = \frac{\Delta q}{3\Delta\varepsilon_s} \tag{1}$$

Here, the shear strain $\varepsilon_s = 2/3(\varepsilon_v - \varepsilon_h)$, ε_v is vertical strain, and ε_h is horizontal strain. In the saturated soil: At the range of ε_s <0.001%, there is a trend that smaller *K* consolidated soil has greater G_{sec} (comprehensive discussion is conducted in the next section). However, at the greater shear strain range, the trend is reversed, that is, smaller *K* consolidated soil has smaller G_{sec}. In the unsaturated soil: At the range of ε_s <0.001%, the difference in G_{sec} is slight (comprehensive discussion is conducted in the next section). At the greater shear strain range, the trend, in which greater *K* consolidated soil has greater G_{sec}, is apparent. Those facts indicate that degradation of G_{sec} with shear strain is greater when *K* or K_{net} is small (the drained monotonic compression starts from a compressional stress state) but it is less when *K* or K_{net} is greater (the drained monotonic compression starts from an extensional stress state).

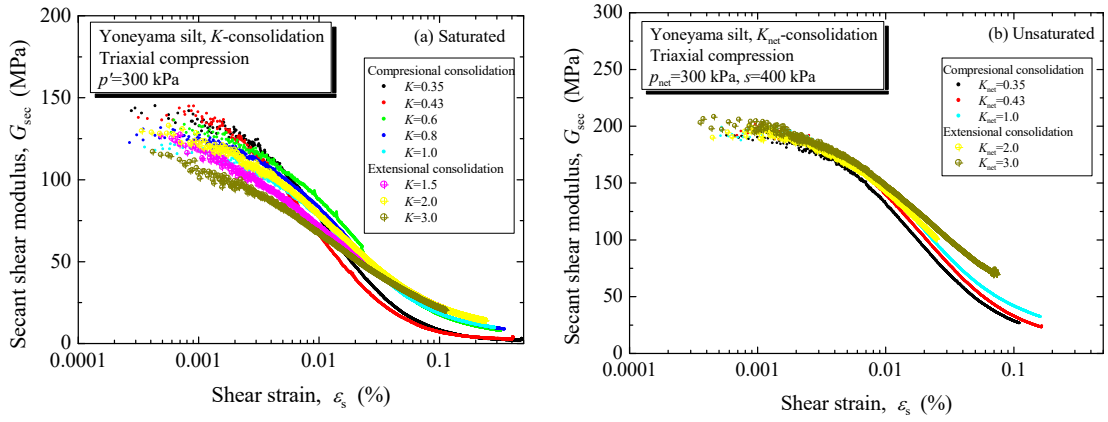

Figure 4. Secant shear modulus in LSS tests (*p'* or p_{net}= 300 kPa): (a) saturated and (b) unsaturated cohesive soils (*s* =400 kPa)

3.2. Effects of *K* or K_{net}-consolidation on G_0

3.2.1. Experiment results

Figure 5(a) shows G_0 of saturated cohesive soil obtained from both BE and LSS tests. The results of G_0 of saturated cohesive soil were similar for both LSS and BE tests. Compressional consolidation (K<1.0): G_0 increases concomitantly with the decrease of K from 1.0 to 0.43, after which it declines at K=0.35. Consequently, the peak appears at around K=0.43, which is coincident with K_0 (=0.43) of Yoneyama silt, as reported in Toyota et al. (2014). K_0 is just the threshold K value, which divides positive (compression) horizontal strain region (K>K_0) and negative horizontal strain region (K<K_0) during K-consolidation.

Extensional consolidation (K>1.0): G_0 increases slightly with the increase of K from 1.0 to 2.0 and then declines at greater K (≥3.0). Therefore, G_0 has two peaks at K_0=0.43 and K=2.0. Moreover, G_0 in the compressional consolidation (K<1.0) is greater than that in the extensional consolidation (K>1.0). Except for K≥3.0, G_0 in the anisotropically consolidated cohesive soil ($K \neq 1.0$) is greater than that in isotropically consolidated soil (K=1.0) under the same p' condition.

Regarding unsaturated cohesive soil presented in Fig. 5(b), G_0 is almost independent with the variation of net stress ratio K_{net}, although G_0 declines slightly at K_{net}=0.35. It is noteworthy that the effects of K in G_0 of saturated cohesive soil, as portrayed in Fig. 5(a), diminishes in that of unsaturated cohesive soil because of the application of matric suction (Fig. 5(b)). The values of G_0 are very close between BE and LSS tests. Therefore, G_0 obtained from BE is used as a representative G_0 hereinafter.

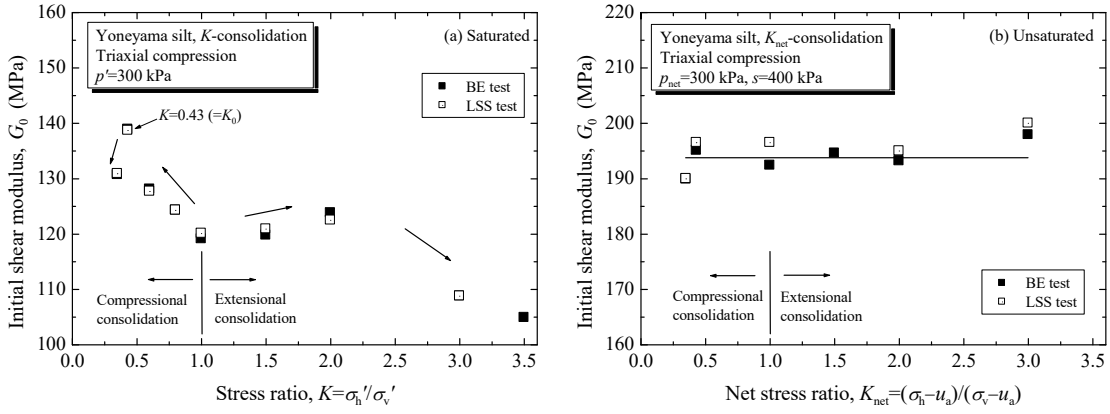

Figure 5. G_0 from LSS and BE tests: (a) saturated and (b) unsaturated cohesive soils

3.2.2. Void ratio effects

G_0 of unsaturated cohesive soils is about 30%–40% greater than that of saturated soils because of the application of matric suction of 400 kPa (comparison between Figs. 5(a) and 5(b)). Void ratios of saturated and unsaturated cohesive soils vary respectively from 0.857 to 0.802 (about 7% variation) and from 0.844 to 0.789 (about 5% variation). Densification occurs during the drying process by the application of suction 400 kPa. Then, K_{net}-consolidation is conducted in the unsaturated specimen, which has stronger stiffness than the saturated soil. Consequently, the void ratios of unsaturated cohesive soil were about 1.0% smaller than those of saturated soil (Le et al.,

2024). To remove the void ratio effects, G_0 was normalized by a void ratio function. Le et al. (2024) investigated the effectiveness for normalization using two kinds of void ratio functions (hyperbolic and exponential forms). The results indicated that the normalized G_0 showed identical trend between two kinds of void ratio functions. Therefore, as the void ratio function, the hyperbolic form, represented by equation (2), was chosen. Value of a=2.973 was used in the equation based on the reports of Hardin and Black (1968) and Hardin and Black (1969).

$$F(e) = \frac{(a-e)^2}{(1+e)} \tag{2}$$

Figures 6(a) and 6(b) show the relation between "normalized G_0" by the void ratio function and stress ratio K for saturated and net stress ratio K_{net} for unsaturated cohesive soils, respectively. The normalized result of saturated soil still exhibits similar trend with Fig. 5(a). Therefore, the effects of K on G_0 are not eliminated merely by using the void ratio function. On the other hand, the G_0 of unsaturated soil is less sensitive to the stress condition (K_{net}-value) than that of saturated soil.

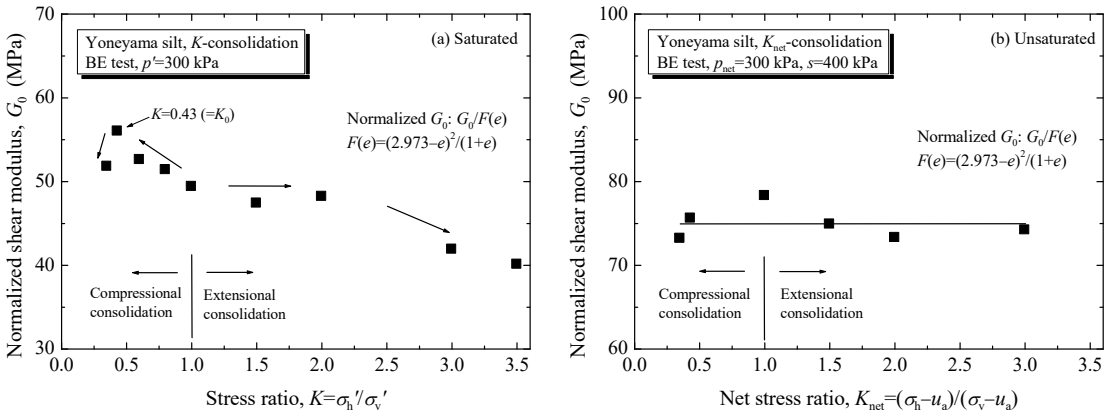

Figure 6. Initial shear modulus normalized by the void ratio

3.2.3. Stress state effects

Hardin and Richart (1963) and Hardin and Drnevich (1972) proposed an empirical expression for G_0, accounting for the effects of effective stress p' and void ratio e:

$$G_0 = AF(e)p_a\left(\frac{p'}{p_a}\right)^n \tag{3}$$

where p_a is the atmospheric pressure of 100 kPa, A and n are fitting parameters, $F(e)$ is the void ratio function, and $p_a(p'/p_a)^n$ is the stress function. For unsaturated soils, p_{net} is used instead of p'.

Aside from the mean effective stress, the importance of individual stress for G_0 was reported by Hardin and Blandford (1989) and Jamiolkowski et al. (1995):

$$G_0 = S_{ij}F(e)OCR^k p_a^{1-n_i-n_j}\sigma'^{n_i}_v\sigma'^{n_j}_h \tag{4}$$

Therein, OCR^k is the OCR function, and $p_a^{1-n_i-n_j}\sigma'^{n_i}_v\sigma'^{n_j}_h$ is the stress function. k is an exponent of OCR that depends on plasticity index I_p. The value of k in Yoneyama silt has been discussed

in Le et al. (2024). Also, i and j are denoted respectively as the direction of the wave propagation/polarization or applied stress direction. n_i and n_j are empirical exponents that respectively account for vertical and horizontal effective stresses. S_{ij} is the dimensionless coefficient. Stokoe et al. (1985), Hardin and Blandford (1989), and Bellotti et al. (1996) reported n_i and n_j as both equal to 0.25. Yu and Richart (1984) also reported that the difference of n_i and n_j between the extension test ($\sigma'_h > \sigma'_v$) and compression test ($\sigma'_v > \sigma'_h$) is extremely small. However, Roesler (1979) insisted that n_i is smaller than n_j under the relation of $n_i + n_j = 0.5$.

G_0 in Fig. 6 is measured under the same p' of 300 kPa for the saturated cohesive soil and the same p_{net} of 300 kPa for the unsaturated cohesive soils, even the K or K_{net}-value is different. The normalized G_0 are varied with the different K-values in the saturated soil (Fig. 6(a)). However, the variation of this kind is slight in the unsaturated soil (Fig. 6(b)). Therefore, p_{net} can be regarded as a good indicator for unsaturated cohesive soil to eliminate the effects of K_{net} using equation (3). However, equation (4) is applied for the saturated soil because equation (3) is insufficient to eliminate the effects of K from the saturated soil.

Figures 7(a) and 7(b) present the normalized G_0 by the void ratio function (2) and the stress function (4) for saturated and the stress function (3) unsaturated soils, respectively. Through the different combinations of n_i and n_j, the best combination was chosen as n_i=0.25 and n_j =0.25 to eliminate the effects of K for saturated cohesive soil (Fig. 7(a)). By contrast, Fig. 7(b) depicts G_0 normalized by equation (3) with n =0.5. Effects of K_{net} for unsaturated cohesive soil can be almost removed. Therefore, individual stresses such as vertical and horizontal normal stresses presented in equation (4) are less important for G_0 of unsaturated cohesive soil. Consequently, to predict G_0 under an anisotropic stress state, net mean stress is effective for unsaturated cohesive soil, while individual normal stresses should be introduced for saturated cohesive soil.

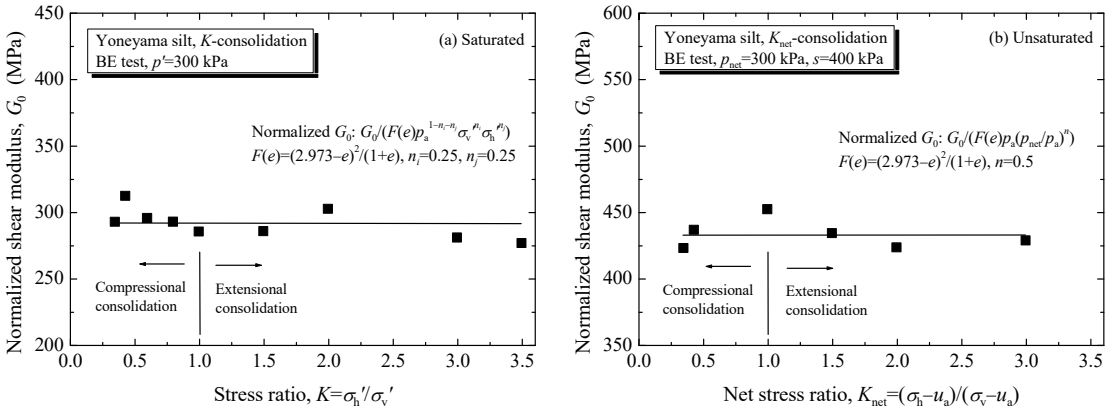

Figure 7. G_0 normalized by the void ratio function and stress function: (a) saturated and (b) unsaturated cohesive soils

4. CONCLUSIONS

Anisotropic shear modulus induced through K or K_{net}-consolidation was investigated using saturated and unsaturated Yoneyama silts. The following conclusions can be drawn from the present study.

1. Very small shear strain: G_0 is strongly affected by anisotropic stress conditions in the saturated cohesive soil under the same p'. G_0 under anisotropic consolidation is greater than that under isotropic consolidation, except for the case of $K \geq 3.0$. In addition, G_0 in the compressional consolidation ($K<1.0$) can have a greater value than that in the extensional consolidation (K>1.0). However, those anisotropic stress effects on G_0 were not significant for the unsaturated cohesive soil because of the effects of matric suction.
2. Shear strain greater than 0.03%: The trends of G_{sec} are changed from the above-mentioned trends of G_0 through the increase of shear strain. With extensional consolidation (K and $K_{net}>1.0$), G_{sec} is greater than that in isotropic consolidation (K and $K_{net}=1.0$). With compressional consolidation (K and $K_{net}<1.0$), G_{sec} is less than that in isotropic consolidation.

The values of G_0 under anisotropic stress conditions are normalized successfully using the void ratio function (2) and the stress function (4) for saturated soil or the stress function (3) for unsaturated soil. Therefore, G_0 under different stress conditions can be inferred from a particular G_0, e.g., in an isotropic stress condition, using those functions.

REFERENCES

Bellotti, R., Jamiolkowski, M., Lo Presti, D. C. F. and O'Neill, D. A. (1996): "Anisotropy of small strain stiffness in Ticino sand," Géotechnique, Vol. 46, No. 1, pp. 115-131.

Casagrande, A. and Carillo, N. (1944): "Shear failure of anisotropic material," J. Boston Soc. Civ. Eng., Vol. 31, No. 4, pp. 74-87.

Chien, L.-K. and Oh, Y.-N. (2002): "Influence of fines content and initial shear stress on dynamic properties of hydraulic reclaimed soil," Canadian Geotechnical Journal, Vol. 39, No. 1, pp. 242-253.

Hao, G. and Lok, T. M. H. (2008): "Study of shear wave velocity of Macao marine clay under anisotropic stress condition," Proc. 14th International Conference on Earthquake Engineering, WCEE, Beijing, China.

Hardin, B. O. and Black, W. L. (1968): "Vibration modulus of normally consolidated clay," Journal of the Soil Mechanics and Foundation Division, ASCE, Vol. 94, No. SM2, pp. 353-369.

Hardin, B. O. and Black, W. L. (1969): "Closure to: vibration modulus of normally consolidated clay," Journal of the Soil Mechanics and Foundation Division, ASCE, Vol. 95, No. SM 6, pp. 1531-1537.

Hardin, B. O. and Blandford, G. E. (1989): "Elasticity of particulate materials," Journal of Geotechnical Engineering, ASCE, Vol. 115, No. 6, pp.788-805.

Hardin, B. O. and Drnevich, V. P. (1972): "Shear modulus and damping in soils: Design equations and curves," Journal of the Soil Mechanics and Foundations Division, Vol. 98, No. SM6, pp.

603-624.

Hardin, B. O. and Richart, F. E., Jr. (1963): “Elastic wave velocities in granular soils,” Journal of the Soil Mechanics and Foundations Division, Vol. 89, No. SM1, pp. 33-65.

JGS 0544 (2020): “Method for laboratory measurement of shear wave velocity of soils by bender element,” Japanese Geotechnical Society standards. (in Japanese)

Jamiolkowski, M., Lancellotta, R. and Lo Presti, D. C. F. (1995): “Remarks on the stiffness at small strains of six Italian clays,” Proceedings of the International Symposium on Pre-failure Deformation of Geomaterials (eds S. Shibuya, T. Mitachi and S. Muira), Vol. 2, pp. 817-836.

Le, N. B., Toyota, H. and Takada, S. (2024): “Small strain shear modulus of saturated and unsaturated cohesive soils under anisotropic consolidations,” Soils and Foundations, Vol. 64, No. 3, 101464, pp. 1-15.

Mitaritonna, G., Amorosi, A. and Cotecchia, F. (2014): “Experimental investigation of the evolution of elastic stiffness anisotropy in a clayey soil,” Geotechnique, Vol. 64, No. 6, pp. 463-475.

Ng, C. W. W., Xu, J. and Yung, S. Y. (2009): “Effects of wetting–drying and stress ratio on anisotropic stiffness of an unsaturated soil at very small strains,” Canadian Geotechnical Journal, Vol. 46, No. 9, pp. 1062-1076.

Rad, N. S. and Clough, G. W. (1984): “New procedure for saturating sand specimens,” Journal of Geotechnical Engineering, Vol. 110, No. 9, pp. 1205-1218.

Rampello, S., Viggiani, G. M. B. and Amorosi, A. (1997): “Small-strain stiffness of reconstituted clay compressed along constant triaxial effective stress ratio paths,” Geotechnique, Vol. 47, No. 3, pp. 475-489.

Roesler, S. K. (1979): “Anisotropic shear modulus due to stress anisotropy,” J. Geotech. Eng. Div. ASCE, Vol. 105, pp. 871-880.

Stokoe, K. H., Lee, S. H. H. and Knox, D. P. (1985): “Shear moduli measurements under true triaxial stresses,” Advances in the Art of Testing Soils Under Cyclic Conditions: Proceedings of a session/sponsored by the Geotechnical Engineering Division in Conjunction with the ASCE Convention in Detroit, Michigan. ASCE, pp. 166-185.

Toyota, H., Sakai, N. and Nakamura, K. (2001): “Mechanical properties of saturated cohesive soil with shear history under three dimensional stress conditions,” Soils and Foundations, Vol. 41, No. 6, pp. 97-110.

Toyota, H., Susami, A. and Takada, S. (2014): “Anisotropy of undrained shear strength induced by K_0 consolidation and swelling in cohesive soils,” International Journal of Geomechanics, Vol. 14, No. 4, pp. 04014019.

Toyota, H., Takada, S. and Susami, A. (2017): “Mechanical properties of saturated and unsaturated cohesive soils with stress-induced anisotropy,” Géotechnique, Vol. 68, No. 10, pp. 1-10.

Yu, P. and Richart, F. E. (1984): “Stress ratio effects on shear modulus of dry sands,” Journal of Geotechnical Engineering, Vol. 110, No. 3, pp. 331–340.